Tapered Multimode Interference Combiners for Coherent Receivers *

Wu Zhigang[1,2], Zhang Weigang[1], Wang Zhi[1], Kai Guiyun[1], Yuan Shuzhong[1], Dong Xiaoyi[1,†], Utaka Katsuyuki[2], and Wada Yasuo[2]

(1 Institute of Modern Optics, Nankai University, Tianjin 300071, China)
(2 School of Science and Engineering, WASEDA University, Tokyo 169-8555, Japan)

Abstract: A new tapered multimode interference (MMI)-based coherent lightwave combiner is reported. A comprehensive theoretical analysis of mode behaviors in the tapered MMI waveguide is presented, and the output characteristics of the tapered MMI combiners with various structures are demonstrated. The combiner is fabricated on a silicon-on-insulator (SOI) substrate. Due to its advantages of having no end-facet reflection, easy extension to a multi-port configuration, high tolerance for fabrication errors, and compact size, the tapered MMI is a good candidate for a coherent lightwave combiner to be used in large-scale photonic integrated circuits.

Key words: integrated optics; multimode interference; combiner; silicon-on-insulator
PACC: 4280; 7820
CLC number: TN256 **Document code:** A **Article ID:** 0253-4177(2006)02-0328-08

1 Introduction

The recent advances in photonic materials and fabrication techniques enable the integration of large-scale photonic circuits. Large-scale photonic integration is necessary for the implementation of sophisticated photonic devices such as delay-line based optical filters and multi-arm Mach-Zenhder interferometers (MZIs)[1~3]. Also, large-scale integration can effectively reduce device cost. Coherent lightwave combiners are indispensable components of large-scale photonic integrated circuits (PIC's). The combiners can be implemented with directional couplers or Y-branch combiners, but directional couplers and Y-branches are usually large and are sensitive to fabrication errors. Moreover, they must be cascaded to make multi-port ($N \times 1$, $N > 2$) coherent lightwave combiners, leading to a larger device size, higher losses and less robustness against fabrication errors. Free-space slab waveguides have been widely used as combiners in array waveguide grating (AWG) devices, but they are wavelength-dependent.

Multimode interference (MMI) couplers, with their compact size, high tolerance for fabrication errors, broad bandwidth characteristics, and polarization insensitivity, have attracted great interest and found many applications as splitters and mode converters[4~6], so they might be expected to used for coherent lightwave combiners. However, back reflections exist in conventional rectangular MMI couplers[7~11]. Figure 1 shows optical power distributions in a rectangular 2×1 MMI combiner, which was simulated with the finite difference beam propagation method (FD-BPM). The bold lines in Fig. 1 are outlines of the simulated MMI combiner with a width of 12μm and length of 395μm. There are two rib single-mode access waveguides at the input and one rib single-mode access waveguide at the output. Considering the single-mode conditions in the rib structure[12], we select the access waveguide with a width and refractive indices of a core and a clad of 2, 3.35, and 3.34μm, respectively.

In the case of in-phase inputs (no relative phase difference between two inputs), even-modes are excit-

* Project supported by the National Natural Science Foundation of China (No. 60577018) and the Key Laboratory of Opto-Electronic Information Science and Technology (Nankai University, Tianjin University) of the Ministry of Education of China (No. 2005-06)
† Corresponding author. Email: xydong@eyou.com, zhangwg@nankai.edu.cn
Received 30 August 2005, revised manuscript received 9 November 2005

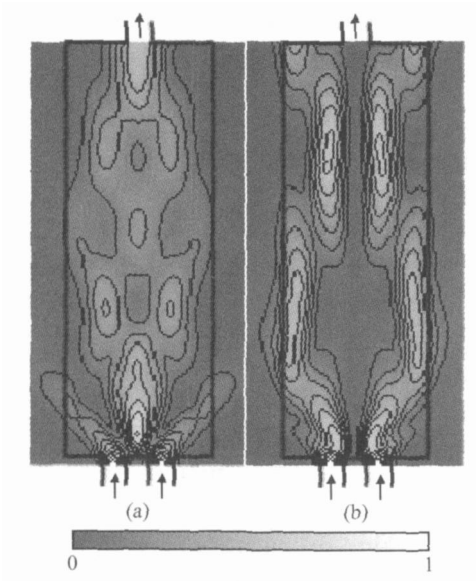

Fig. 1　Power distributions in an MMI coupler with a rectangular shape in the case of in-phase inputs (a) and out-of-phase inputs (b)

ed in the MMI section because of the symmetric inputs. As a result of multimode interference, a single-mode interference image appears at a position determined by the effective width and refractive index of the MMI waveguide. The image can be extracted by forming an output waveguide at the position, as shown in Fig. 1(a). When there is a relative phase difference between the two light inputs, the MMI pattern is changed. In the case of out-of-phase inputs (a relative phase difference of π between two inputs) only odd-modes are excited. So the MMI pattern at the output is reversed compared to that of the in-phase inputs. No modes can be coupled into the output waveguide, and most of the power is concentrated in the MMI shoulders, the facet wall, as shown in Fig. 1(b). Consequently, there is a large end-facet reflection. According to our simulation, the reflection back into an input port is - 16dB when the end-facet reflectivity is 25 %. This simulated result is larger than the experimental result of - 25dB for a 2 ×2 MMI splitter[8,9]. The reason is that the output power of a 2 ×1 MMI combiner with out-of-phase inputs is concentrated on the facet wall, while the output power of a 2 ×2 MMI splitter is concentrated on the output ports. Especially when the MMI is deeply etched or covered by a metal layer, the reflection is more severe. The reflection may not be a problem for some passive systems. However, when the combiner is connected with a semiconductor optical amplifier (SOA) or a laser, the reflection will degenerate the system performance. In order to minimize the end-facet reflection, several methods have been reported[10,11]. Previously we proposed another method using a tapered MMI combiner to avoid the back reflection[13,14].

Tapered MMIs with two symmetric end-facets have been reported as compact power splitters[15~18], but tapered MMIs with asymmetric end-facets for power combiners have not been reported. Actually, MMI coherent lightwave combiners are different from MMI splitters, although it seems that MMI splitters can be used as combiners by introducing light propagating in the opposite direction. In the case of MMI coherent lightwave combiners, relative phase changes of input lights will change the power distribution in an MMI section.

In this paper we present theoretical analysis of and experimentation with tapered MMI coherent lightwave combiners.

2　Theoretical analysis

2.1　Multimode interference images in tapered MMI waveguides

The tapered MMI combiner is schematically shown in Fig. 2, in which the combiner length, the initial MMI width, the access waveguide width, and the access waveguide spacing are denoted by L, W, ww, and ws, respectively. The combiner output end and the output waveguide have the same width. The tilted and curved borders can be any shape such as an arc or an exponential curve.

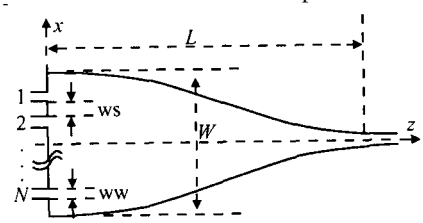

Fig. 2　Schematic diagram of a tapered MMI-based combiner

The fundamental operation principle in the tapered waveguide is the same as that of conventional MMI couplers[19]. By introducing input light from a single-mode access waveguide, several modes are excited in the MMI section. However, the number of the excited modes decreases during propagation in the combiner due to the tapered structure, and there is only a single mode at the

output. Since the number of supported modes decreases, an interference image in the tapered MMI results only from those modes supported at the position with a local waveguide width. We call these the effective modes of the image. High-order modes disappear during propagation in the tapered MMI, but the power loss can be kept small if the taper is not steep. As we discuss later, the low loss comes mainly from the power conversion from high-order modes to low-order modes because of the interference of the hybrid modes.

In a conventional MMI coupler with a rectangular shape, the propagation constant spacing is derived as[4]

$$\beta_0 - \beta_v \approx \frac{v(v+2)\pi\lambda_0}{4nW^2} \quad (1)$$

where W is the effective width of the MMI waveguide with a refractive index of n, λ_0 is the free-space wavelength, and v is the mode number. Since the propagation constant spacing is independent of the propagation position, there always exist positions where the phase differences of all high-order modes and the fundamental mode are the same —— for example, $2l\pi$ (self-image, l is an integer). Therefore stable and clear images periodically appear along the propagation in the MMI waveguide. The images are stable and clear because they are generated by the contribution of all modes in the MMI section.

For the tapered MMI, W is not a constant, so the propagation constant spacing given by Eq. (1) depends on position. In other words, the border shape determines the propagation constant spacing. In order to analyze the mode propagation characteristics, we deduced the propagation constant spacing in the tapered MMI waveguide[4,15]. The dispersion relation at any position z can be written as

$$(nK_0)^2 = K_{xv}(z)^2 + \beta_v(z)^2 \quad (2)$$

where $K_{xv}(z)$ and $\beta_v(z)$ are the lateral wavenumber and propagation constant of the mode v at position z, respectively, and K_0 is a free-space wavenumber. The lateral wavenumber is given by

$$K_{xv}(z)\,W(z) = (v+1)\pi \quad (3)$$

where W(z) is the effective MMI width at the position z, and v is a mode number such as 0, 1, ⋯, m - 1, m, where m is the number of effective modes.

By analogy with Eq. (1), the propagation constant spacing from the v-th mode to the fundamental one with propagation constants of $\beta_v(z)$ and $\beta_0(z)$ can be expressed as

$$\beta_0(z) - \beta_v(z) \approx \frac{v(v+2)\pi\lambda_0}{4nW(z)^2} \quad (4)$$

where the effective width W(z) depends on the tapered MMI position.

The relative phase difference $\Delta\phi_v$ after propagation from position z_1 to z_2 in the tapered section is give by[14]

$$\Delta\phi_v(z_1, z_2) = \int_{z_1}^{z_2} (\beta_0(z) - \beta_v(z))\,dz = \frac{v(v+2)\pi\lambda_0}{4n}\int_{z_1}^{z_2}\frac{dz}{W(z)^2} \quad (5)$$

Equation (5) shows that the relative phase difference per unit length $\Delta\phi_v(z_1, z_2)/(z_2 - z_1)$ depends on the propagation position, which is quite different from a conventional rectangular MMI waveguide. So the question is whether there exist positions in the tapered MMI where the relative phase differences of all the modes to the fundamental mode are the same, for example $2l\pi$ (l is an integer). If such positions do not exist, stable and clear interference images cannot exist in the tapered MMI.

The ratios α_v of relative phase differences of the v-th and 1st modes to the fundamental mode propagated from the position z_1 to z_2 can be written as

$$\alpha_v = \frac{\Delta\phi_v(z_1, z_2)}{\Delta\phi_1(z_1, z_2)} = \frac{v(v+2)}{3} \quad (6)$$

Equation (6) describes an important characteristic of mode propagation in a tapered MMI waveguide. Although every mode has a different phase difference from the fundamental mode in different propagation sections, the phase differences of all modes proportionally change in a propagation section. We suppose there are m effective modes with respective phases of

$$\phi_0(0), \phi_1(0), \cdots, \phi_{m-1}(0) \quad (7)$$

at an initial position. We can slice the taper into many small segments. By Eq. (6), the phases of the effective modes past the first slice can be written as

$$\phi_0(1), \phi_1(1), \cdots, \phi_v(1) = \alpha_v(\phi_1(1) - \phi_0(1)) + \phi_0(1) \quad (8)$$

where $v = 2, 3, \cdots, m-1$. Past slice k, the phases of these effective modes can be written as

$$\begin{aligned} &\text{Mode } 0: \psi_0 = \phi_0(0) + \phi_0(1) + \cdots + \phi_0(k) \\ &\text{Mode } 1: \psi_1 = \phi_1(0) + \phi_1(1) + \cdots + \phi_1(k) \\ &\text{Mode } v: \psi_v = \alpha_v(\psi_1 - \psi_0) + \psi_0 \end{aligned} \quad (9)$$

Since we are only interested in the phases of

higher modes relative to the fundamental one, we can rewrite Eq. (9) as

$$0, (\psi_1 - \psi_0), 8(\psi_1 - \psi_0)/3, \cdots, \nu(\nu+2)(\psi_1 - \psi_0)/3 \quad (10)$$

for mode 0, mode 1, mode 2, ···, mode ν. Thus, the self-images appear at the positions where $\psi_1 - \psi_0 = 6l\pi$, l is an integer. Thus, the positions that give specific phase differences exist even in the tapered MMI. If the border shape W(z) is known, the positions L of self-images can be obtained by

$$\int_0^L \frac{dz}{W(z)^2} = \frac{8nl}{\lambda_0} \quad (11)$$

Equation (11) shows that the self-image spacing depending on the border shape is a chirped period, which is different from that of conventional rectangular MMI waveguides.

2.2 Free of end-facet reflection

In Fig. 1, there is a severe end-facet reflection for the rectangular MMI with out-of-phase inputs. Under the same conditions, we simulated the characteristics of the tapered MMI with arc borders, as shown by the bold lines in Fig. 3. In the case of in-phase inputs, only even-modes are excited because of the symmetric inputs. The clear single-mode image generated is coupled into the output waveguide, and the loss is small, as shown in Fig. 3(a).

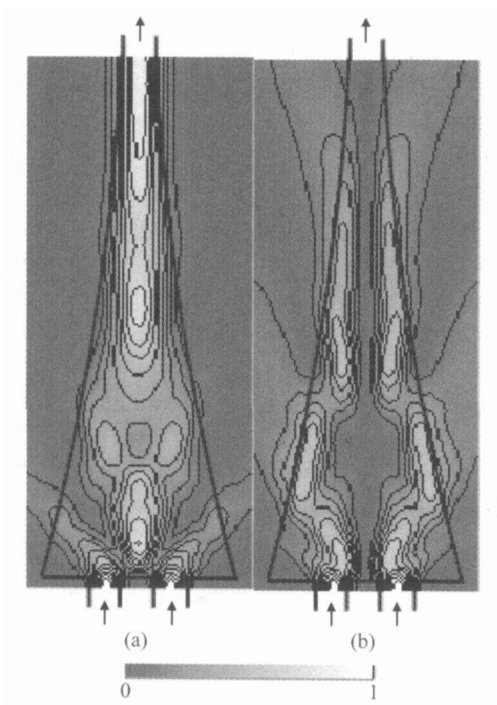

Fig. 3　Power distributions of a tapered MMI combiner in the cases of in-phase inputs (a) and out-of-phase inputs (b)

In the case of out-of-phase inputs, by which we mean asymmetric inputs, only odd-modes are excited. So there is no power distribution on the centerline as shown in Fig. 3(b). No output is extracted from a centered single-mode waveguide. High-order odd-modes leak out of the tapered structure. Therefore, the device is free of the end-facet reflection problem mentioned above.

2.3 Extinction ratios in various structures

The output extinction ratio of a coherent lightwave combiner is a basic characteristic of its performance. The extinction ratio of the tapered combiner is affected by its structural properties such as the radius of curvature R of the borders, the access waveguide spacing ws, and the device length L, as shown in Fig. 4, which are simulated by FD-BPM. The border shape of the 2 ×1 tapered combiner used here is an arc with radius R.

For a tapered MMI with a given initial width and length, R strongly affects the extinction ratio. The mechanisms are as follows. In the case of in-phase inputs, all the excited modes are even-modes, and the interference images tend to concentrate along the taper centerline, as shown in Fig. 3(a), so the high-order modes have low loss. That is why the excess loss of a 2 ×1 MMI coupler with in-phase inputs is less than that of the same 2 ×1 MMI coupler with one-port input. On the other hand, in the case of out-of-phase inputs, only odd-modes are excited, and the generated MMI images are concentrated on the sides, as shown in Fig. 3(b), and almost all of the high-order modes leak out of the combiner due to the taper structure. These phenomena lead to a larger extinction ratio. These mechanisms explain that smaller R tends to lead to larger loss for high-order modes and a large extinction ratio, as shown in Fig. 4(a). The diamonds, squares, and triangles are the output powers of tapered combiners for R = 22.5, 40mm, and infinity, with structure parameters of W = 6μm, ws = 2μm, and L = 300μm. The excess losses defined as the output in the case of in-phase inputs are nearly the same for different R, so a smaller R is better. However, a very small R is impractical because of severe scattering loss or no passage through the MMI section. So R must be not less than the minimum radius R_{min} defined as

$$R_{min} = \frac{(W - ww)^2 + 4L^2}{4(W - ww)} \quad (12)$$

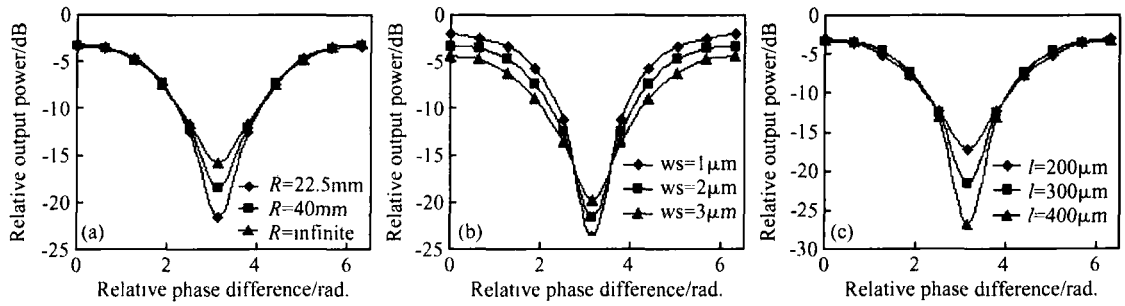

Fig. 4 Relative output power as a function of relative phase difference of two inputs under various parameters (a) Border curvature radii; (b) Access waveguide spacing; (c) Device length

where W, ww, and L are the initial width, the access waveguide width, and the length of the tapered MMI. For R_{min}, the arc is tangential to the output waveguide, so there is no joint loss between the MMI section and the output waveguide. In this sense, R_{min} is an optimal curvature radius, which our simulated results confirm[13].

The access waveguide spacing ws affects the device performance largely as shown in Fig. 4(b). The curves with diamonds, squares, and triangles are the output powers of the tapered combiners with L = 300μm and R = R_{min}. W = 5, 6, and 7μm are adopted corresponding to ws values of 1, 2, and 3μm, respectively. The smaller access waveguide spacing yields a larger extinction ratio and a small excess loss. The large excess loss for the larger access waveguide spacing is caused by two factors: One is the spurious mode conversion from the tapered structure; the other is that the excited modes are different depending on the access waveguide spacing. However, the smallness of the access waveguide spacing is limited by fabrication techniques and coupling between access waveguides.

Figure 4(c) shows the simulated output powers of tapered combiners for the device lengths L of 200, 300, and 400μm, with the structure parameters W = 6μm, ws = 2μm, and R = R_{min}. A longer device leads to a larger extinction ratio due to greater losses of high-order modes. Therefore a long tapered MMI combiner is necessary for a desired extinction ratio, although compactness is one of the advantages of the tapered structure[15]. Figure 5 shows the dependence of extinction ratios on the device length and the excess loss of a 2 ×1 tapered MMI combiner with the structure parameters R = R_{min}, ww = 2μm, ws = 1μm, and W = 5μm. Therefore, the device length is actually determined by balancing the desired extinction ratio, excess loss, and compactness. For example, when the desired extinction ratio is larger than 15dB, the device length should not be less than 140μm.

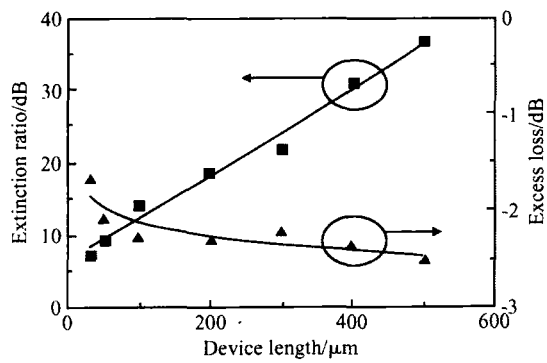

Fig. 5 Dependence of extinction ratios and excess loss on tapered MMI length

The insertion loss comes mainly from the scattering loss by the two MMI curved borders in the case of in-phase inputs. The scattering loss depends on the border shape and the distribution of the excited modes in the taper. So we can improve the excess loss by forming the images of the excited modes as close to the centerline of the tapered MMI as possible, which can be realized by reducing the input access waveguide spacing, as shown in Fig. 4(b).

3 Fabrication and assessment

3.1 Performance of tapered MMI combiners

The 2 ×1 tapered MMI combiners are fabricated on a silicon-on-insulator (SOI) substrate with a top silicon layer of 1.6μm and SiO_2 layer of 1μm. First, a Cr-layer with a thickness of 0.15μm was deposited on the wafer. Next, a photo-mask

pattern was transferred to the Cr-layer by standard photolithography and wet etching. The Cr pattern will serve as a mask for etching the waveguide layer. The rib waveguides with a width of 2μm were etched to 0.6μm by reactive ion-beam etching utilizing a C_3F_8-O_2 gas mixture. After the etching process, a 0.14μm SiO_2 layer was deposited on the wafer. Finally the wafer was cleaved for measurement after chemical mechanical polishing (CMP).

In order to assess a 2 ×1 tapered MMI combiner, the ASE source was input into the access waveguides by a 3dB fiber coupler with TE polarization. The fiber coupler and the combiner formed an asymmetric MZI. The extinction ratio and the insertion loss of the combiner are about 10 and - 14dB, as shown in Fig. 6. The transmission loss of the straight waveguides in our experiments is about 0.7dB/mm, obtained by cutback measurements, which was mainly from the sidewall roughness of the etched waveguides. The excess loss of the tapered MMI combiner is experimentally evaluated to be about 2dB, which is a little larger than the result of 1.6dB simulated by FD-BPM. An evaluation of the reflection characteristics of the combiner is reported elsewhere[20].

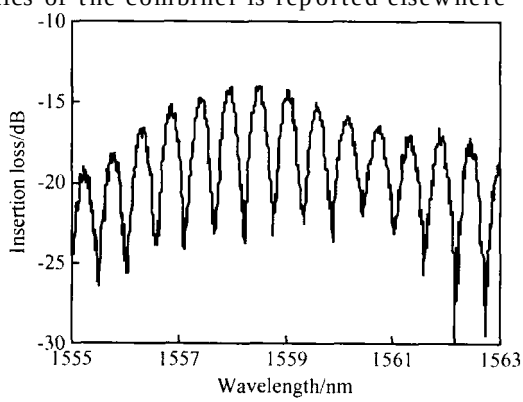

Fig. 6　Experimental assessment of a tapered MMI combiner

3.2　MZI modulators with a 2 ×1 tapered MMI combiner

As an application, we fabricated symmetric MZI modulators with the tapered MMI combiner on a SOI substrate. Unlike the MZI modulator with a rectangular MMI combiner, the new MZI modulator has no backed inner reflection. So it is better used as a cross-phase modulation (XPM)-based high-speed MZI modulator by inserting a SOA into one arm. The SOI substrate and fabrication processes are the same as that mentioned above. After the fabrication of the MZI, a 0.5μm Cr metal heater, which served as a phase shifter, is formed on one arm of the MZI, as shown in Fig. 7. The power splitter in the MZI is a 3dB rectangular MMI coupler. The initial width and length of the tapered MMI combiner are 5.2 and 500μm, respectively, as shown in the SEM picture in the figure. The size of the MZI modulator is 5mm × 0.6mm.

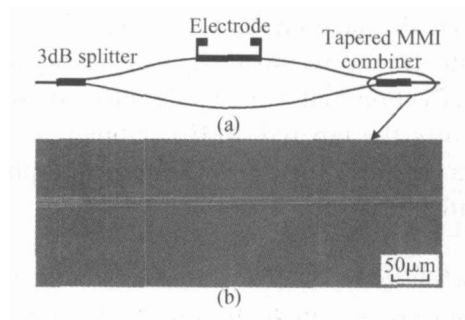

Fig. 7　(a) Schematic of a MZI; (b) SEM photograph of the tapered MMI combiner

The measured results are shown in Fig. 8. The dotted line and the solid triangles are for the simulated and measured results of the TE mode, respectively. The insertion loss is about - 28.2dB. The smaller modulation depth as compared with the result in Fig. 6 results mainly from the unbalanced output of the 3dB splitter in the MZI. The measured results agree with the simulated results, although there is a little shift when the heater power is high. We believe the shift occurs because the whole wafer is heated, but it can be removed by bonding the wafer or forming a trench between the two MZI arms[21].

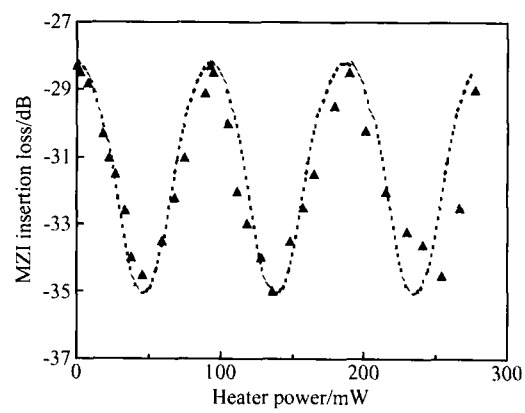

Fig. 8 Simulated and experimental results

4 Conclusion

We analyzed the characteristics of tapered MMI-based coherent lightwave combiners and theoretically confirmed that stable and clear MMI images exist in the tapered MMI section. The generated MMI images in the tapered MMI combiner show a chirped periodicity. We simulated the output characteristics of 2 ×1 tapered MMI coherent lightwave combiners with various structures to find the optimal design. We experimentally demonstrated the tapered MMI combiners on a SOI substrate. Due to its advantages of having no end-facet reflection and a high tolerance for fabrication errors, the tapered MMI combiner is promising as a coherent lightwave combiner in photonic integrated circuits.

Acknowledgement The authors would like to show sincere gratitude to the Nano-Foundry of Nano-Tech Research Center (NTRC) of WASEDA University for their experimental support.

References

[1] Moslehi B, Goodman J W. Novel amplified fiber-optic recirculating delay line processor. J Lightwave Technol, 1992, 10: 1142

[2] Doerr C R, Stulz L W, Levy D S, et al. Wavelength add-drop node using silica waveguide integration. J Lightwave Technol, 2004, 22: 2755

[3] Paiam M R, MacDonald R I. A 12-channel phased-array wavelength multiplexer with multimode interference couplers. IEEE Photonics Technol Lett, 1998, 10: 241

[4] Soldano L B, Pennings E C M. Optical multi-mode interference device based on self-imaging: principles and applications. J Lightwave Technol, 1995, 13: 615

[5] Lee B, Shin S. Mode - order converter in a multimode waveguide. Opt Lett, 2003, 28: 1660

[6] Leuthold J, Hess R, Eckner J, et al. Spatial mode filters realized with multimode interference couplers. Opt Lett, 1996, 21: 836

[7] Pennings E C M, Van Roijen R, Van Stralen M J N, et al. Reflection properties of multimode interference devices. IEEE Photonics Technol Lett, 1994, 6: 715

[8] Shibata Y, Oku S, Yamamoto M, et al. Quantitative analysis of optical reflection in a multimode interference 3dB coupler using a low-coherence interferometric. Electron Lett, 1996, 32: 2266

[9] Erasme D, Spiekman L H, Herben C G P, et al. Experimental assessment of the reflection of passive multimode interference couplers. IEEE Photonics Technol Lett, 1997, 9: 1604

[10] Gottesman Y, Rao E V K, Dagens B. A novel design proposal to minimize reflections in deep-ridge multimode interference couplers. IEEE Photonics Technol Lett, 2000, 12: 1662

[11] De Merlier J, Morthier G, Verstuyft S, et al. Experimental demonstration of all-optical regeneration using an MMI-SOA. IEEE Photonics Technol Lett, 2002, 14: 660

[12] Soref R A, Schmidtchen J, Petermann K. Large single-mode rib waveguides in GeSi-Si and Si-on-SiO_2. IEEE J Quantum Electron, 1991, 27: 1971

[13] Wu Z, Utaka K. Horn-shaped multimode interference-based N ×1 combiner. CLEO/PR, Taiwan, 2003

[14] Wu Z, Utaka K. Study on tapered multimode interference-based coherent lightwave combiners. IEICE Trans Electron, 2005, E88-C: 1005

[15] Levy D S, Scarmozzino R, Osgood J R. Length reduction of tapered N ×N MMI devices. IEEE Photonics Technol Lett, 1998, 10: 830

[16] Wei H, Yu J, Zhang X, et al. Compact 3-dB tapered multimode interference coupler in silicon-on-insulator. Opt Lett, 2001, 26: 878

[17] Levy D S, Scarmozzino R, Li Y M, et al. A new design for ultracompact multimode interference-based 2 ×2 couplers. IEEE Photonics Technol Lett, 1998, 10: 96

[18] Wei H, Yu J, Liu Z, et al. Signal bandwidth of general N ×N multimode interference couplers. J Lightwave Technol, 2001, 19: 739

[19] Ulrich R, Ankele G. Self-imaging in homogeneous planar optical waveguides. Appl Phys Lett, 1975, 27: 337

[20] Wu Z, Nakamura K, Honda S, ea al. Implementation of tapered multimode interference lightwave combiner on silicon-on-insulator substrate with negligible back-reflection. Jpn J Appl Phys, 2005, 44: L923

[21] Lai Q Hunziker W, Melchior H. Low-power compact 2 ×2 thermooptic silica-on-silicon waveguide switch with fast response. IEEE Photonics Technol Lett, 1998, 10(5): 681

用于相干接收的锥形多模干涉合波器*

武志刚[1,2]　张伟刚[1]　王　志[1]　开桂云[1]　袁树中[1]　董孝义[1,†]
宇高胜之[2]　和田恭雄[2]

(1 南开大学现代光学研究所，天津　300071)
(2 早稻田大学理工学部，东京　169-8555，日本)

摘要：报道了一个新的基于锥形多模干涉的相干光波合波器.对锥形多模波导中的模式行为给出了完整的理论分析,并给出了该锥形合波器在不同结构下的输出特性.在一个绝缘体上硅的基板上实现了该器件.鉴于无后向反射,容易扩展为多口配置,对实验误差有大的允许度和尺寸紧凑等优点,这种锥形多模干涉的合波器是大型光子集成中所用的相干光波合波器的理想选择.

关键词：集成光学；多模干涉；合波器；绝缘体上硅
PACC：4280；7820
中图分类号：TN256　　**文献标识码**：A　　**文章编号**：0253-4177(2006)02-0328-08

*国家自然科学基金(批准号:60577018)和光电信息技术科学教育部重点实验室(南开大学,天津大学)(批准号:2005-06)资助项目
† 通信作者. Email:xydong@eyou.com,zhangwg@nankai.edu.cn
2005-08-30 收到,2005-11-09 定稿